

Ostwald Ripening Behavior of Al_8CeCu_4 Phase in Al-14Cu-7Ce Alloy

Li Hai^{1,2}, Xu Wei¹, Wang Zhixiu^{1,2}, Fang Bijun^{1,2}, Song Renguo^{1,2}, Zheng Ziqiao³

¹ Changzhou University, Changzhou 213164, China; ² Jiangsu Key Laboratory of Materials Surface Science and Technology, Changzhou 213164, China; ³ Central South University, Changsha 410083, China

Abstract: The Ostwald ripening behavior of Al_8CeCu_4 phase in the Al-14Cu-7Ce alloy annealed at elevated temperatures was investigated using hardness testing, scanning electron microscopy, image analyses and physical modeling. Results indicate that the average radius of Al_8CeCu_4 particles increases while the hardness of the alloy decreases with increasing of annealing temperature and time. The ripening process of Al_8CeCu_4 phase is mainly controlled by the volume diffusion of Ce. The ripening kinetic of Al_8CeCu_4 particles satisfies well the modified Lifshits-Slyozov-Wagner theory, taking into account the effect of the volume fraction of Al_8CeCu_4 particles. The volume diffusion coefficient of Ce and the interfacial energy between the matrix and Al_8CeCu_4 phase were also calculated based on the general rate equation.

Key words: Al-14Cu-7Ce alloy; Ostwald ripening; Al_8CeCu_4 phase

According to the Gibbs-Thompson relation, the equilibrium concentration of the solute atoms around the interfaces of smaller particles is larger than that around larger particles and thus a concentration gradient is formed, which results in the growth of larger particles at the expense of smaller ones. This process is the so-called Ostwald ripening, which finally alters the average size and the size distribution of particles. The nature, the size, the size distribution and the morphology of second phase particles in metallic materials are an important issue which will affect the mechanical properties, the plastic deformability, the recovery and the recrystallization of deformed grains and subsequent grain growth. Therefore, it is of great importance to study the Ostwald ripening behavior of second phase particles^[1-5].

According to the pseudo-binary Al- Al_8CeCu_4 phase diagram (Fig.1)^[6,7], Al-14Cu-7Ce alloy belongs to the one with eutectic composition which results in good castability of the alloy. The typical as-cast microstructure of Al-14Cu-7Ce alloy consists of fine lamellar α -Al and Al_8CeCu_4 phase after chill casting^[8,9]. The previous results showed that the as-cast

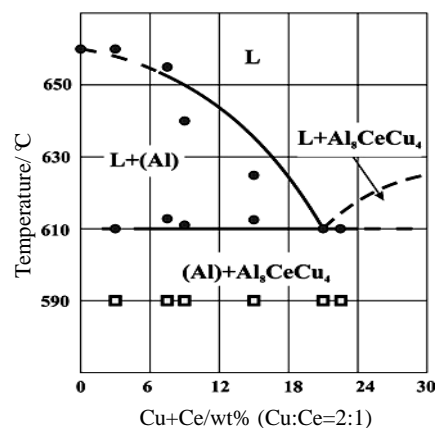


Fig.1 Pseudo-binary Al- Al_8CeCu_4 phase diagram^[6]

Al-14Cu-7Ce alloy had good heat resistance^[6,8-10]. Furthermore, the lamellar Al_8CeCu_4 phase would spheroidize to lower the interfacial energy between Al_8CeCu_4 phase and Al matrix upon annealing at elevated temperatures, which finally resulted in good plastic deformability of the alloy. At the same

Received date: May 25, 2015

Foundation item: National Natural Science Foundation of China (51301027, 51571038); the Natural Science Foundation of Jiangsu Higher Education Institutions of China (14KJB430002); the Natural Science Foundation of Jiangsu Province (BK20151188)

Corresponding author: Wang Zhixiu, Ph. D., Lecturer, School of Material Science and Engineering, Changzhou University, Changzhou 213164, P. R. China, Tel: 0086-519-86330069, E-mail: Xiu_wzx@163.com

Copyright © 2016, Northwest Institute for Nonferrous Metal Research. Published by Elsevier BV. All rights reserved.

time, the wrought alloy still retained good heat resistance^[8-10].

For the variation of average radius of the Al_8CeCu_4 particles during annealing exerts a great effect on the subsequent plastic deformation and mechanical properties, the Ostwald ripening behavior of the spheroidized Al_8CeCu_4 particles will be investigated in the present work. Meanwhile, the kinetic equation in the form of LSW (Lifshits-Slyozov-Wagner) theory, in which the effect of the volume fraction of the Al_8CeCu_4 particles is taken into consideration, will also be developed.

1 Experiment

The experimental alloy ingots with chemical composition of 14Cu, 7Ce and balance Al (wt%) were prepared using chill casting in the laboratory.

To understand the microstructural characteristics of the alloy ingot, the DSC tests were carried out using samples of $\Phi 5 \text{ mm} \times 1 \text{ mm}$ with a heating rate of $10 \text{ }^\circ\text{C}/\text{min}$ in the argon atmosphere.

Slices of $10 \text{ mm} \times 10 \text{ mm} \times 3 \text{ mm}$ were cut from the castings. The slices were previously annealed at 740 K for 120 h to achieve the complete spheroidization of the lamellar Al_8CeCu_4 phase. Then the as-spheroidized samples were further annealed at 773, 803, 833 and 863 K, with an interval of 20 h to 120 h. Vickers hardness of the annealed samples was measured by a HVS-5Z unit at a load of 0.5 kg to study the influence of annealing conditions on mechanical property. The Vickers hardness presented here was the average of at least 10 values. Microstructural morphologies of the annealed samples were observed by a JSM-6510 scanning electron microscopy (SEM), and the average radius of the Al_8CeCu_4 particles was quantitatively measured using a TCI-1000 image processing software. At least 1000 Al_8CeCu_4 particles were counted for each annealing condition to ensure the reliability of the average radius.

2 Results and Discussion

2.1 Microstructure

The SEM morphology of the as-cast Al-14Cu-7Ce alloy is shown in Fig.2. The typical eutectic microstructure consists of lamellar $\alpha\text{-Al}$ and Al_8CeCu_4 phase. Based on the image analysis, the volume fraction of Al_8CeCu_4 phase is determined

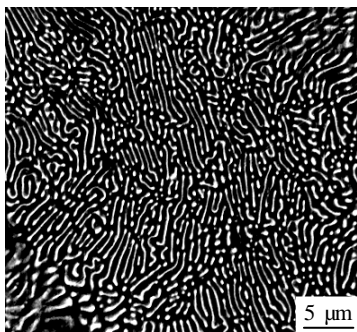


Fig.2 SEM image of the Al-14Cu-7Ce ingot

to be about 24 vol%, which is in good agreement with the result reported by Belov et al^[6]. The lamellar space and the thickness of Al_8CeCu_4 phase are about $1 \text{ }\mu\text{m}$ and 400 nm , respectively. From Fig.3, only one endothermic peak is observed in the DSC curve of the ingot and according to the extrapolation method the starting melt point is determined to be $611 \text{ }^\circ\text{C}$, which is very close to the eutectic point of the Al-14Cu-7Ce alloy ($610 \text{ }^\circ\text{C}$)^[6]. Such result verifies again that the ingot microstructure consists of the eutectic $\alpha\text{-Al}$ and Al_8CeCu_4 phase.

After the Al-14Cu-7Ce alloy slices were previous annealed at 743 K for 120 h, the lamellar Al_8CeCu_4 phase was spheroidized completely, and the average radius of Al_8CeCu_4 particles is about 230 nm, as shown in Fig.4a. The spheroidization kinetics and mechanism of the lamellar Al_8CeCu_4 phase will be presented elsewhere.

Based on the previous annealing treatment, the alloy was further annealed at 773, 803, 833 and 863 K with an interval of 20 h to 120 h. The SEM morphologies of the alloy after annealing for 120 h are shown in Fig.4b~4e. The measured average radii of the obtained Al_8CeCu_4 particles are about 306, 365, 428, and 498 nm. Fig.5 shows the change of average radius of Al_8CeCu_4 particles with the annealing temperature and time, which indicates that the average radius of Al_8CeCu_4 particles increases with increasing of the annealing temperature. Since the growth of Al_8CeCu_4 particles during annealing is a thermal diffusion process of atoms in the matrix for a given metallic system, which is mainly influenced by two factors of annealing temperature and time, and the exponential influence of temperature is more pronounced according to the Arrhenius equation.

2.2 Hardness

Fig.6 shows the variation of Vickers hardness of Al-14Cu-7Ce alloy, which was previously annealed at 743 K for 120 h and then annealed at 773, 803, 833 and 863 K. After previous annealing at 743 K for 120 h, the initial hardness $\text{HV}_{0.5}$ of the alloy is 835 MPa. The hardness of the alloy decreases gradually at 4 annealing temperatures, in which no incubation period exists as described by Atasoy et al^[11]. With the increase of annealing time, all the curves can be almost divided into two regions with different slopes, in which the values of

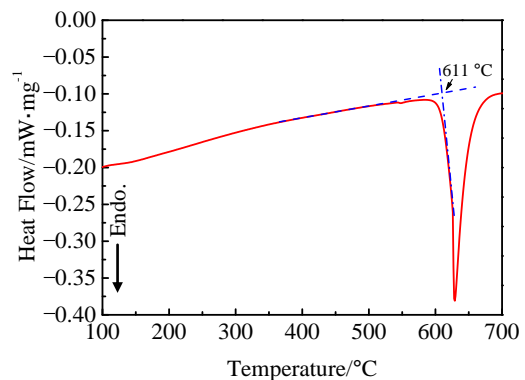


Fig.3 DSC thermogram of the Al-14Cu-7Ce ingot

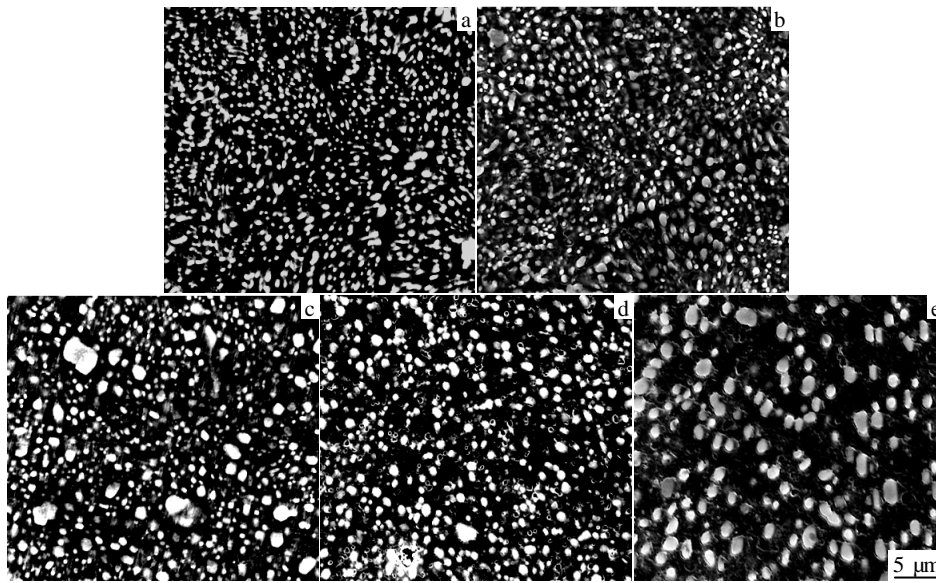


Fig.4 SEM images of the spheroidized Al-14Cu-7Ce alloy after annealing at different temperatures: (a) 743 K/120 h, (b) 743 K/120 h + 773 K/120 h, (c) 743 K/120 h + 803 K/120 h, (d) 743 K/120 h + 833 K/120 h, and (e) 743 K/120 h + 863 K/120 h

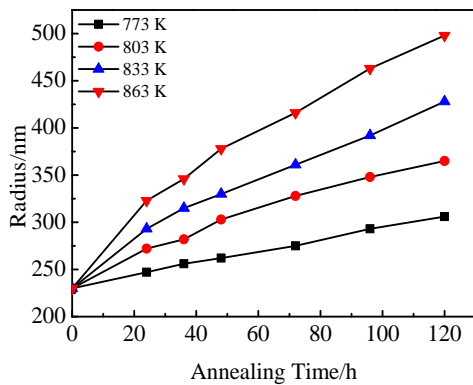


Fig.5 Influences of annealing temperature and time on the average radius of the Al₈CeCu₄ particles in the Al-14Cu-7Ce alloy

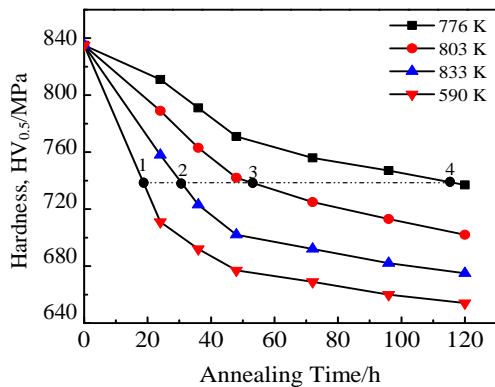


Fig.6 Vickers hardness of the Al-14Cu-7Ce alloy annealed at different temperatures for different time (“1, 2, 3 and 4” in the figure denote the calculating points for the hardness HV_{0.5} = 740 MPa)

hardness decrease quickly before the annealing of 48 h. Furthermore, the higher the annealing temperature is, the quicker the decrease of the values of hardness will be.

The strengthening mechanism of the Al-14Cu-7Ce alloy can be attributed to the formation of the Al₈CeCu₄ particles during the eutectic transformation process, which is different from the conventional age-hardenable aluminum alloys, such as Al-Cu-Mg alloys and Al-Zn-Mg alloys^[12], in which the precipitation of nano-scale precipitates during artificial ageing takes major effect in their strengthening. Because the volume fraction of Al₈CeCu₄ phase remains unchangeable during the annealing process, the size and the number of Al₈CeCu₄ particles will directly influence the mechanical properties of Al-14Cu-7Ce alloy according to the Orowan’s relation. It is seen from Fig.4 and Fig.5 that the average radius of the Al₈CeCu₄ particles increases and their number density decreases with the increase of the annealing temperature and time, which thus lead to the decrease of hardness of the Al-14Cu-7Ce alloy (Fig.6).

2.3 Ripening kinetics of Al₈CeCu₄ particles

In order to predict the change of the average radius of Al₈CeCu₄ particles during annealing, the classical LSW relation developed by Lifshits and Slyozov^[13], Wagner^[14] is used as follows:

$$R_t^3 - R_0^3 = Kt = 8D\sigma V_p^2 C_m / 9RTV_m C_p t \quad (1)$$

For the Al-14Cu-7Ce alloy, R_0 is the initial average radius of Al₈CeCu₄ particles, which is about 230 nm after annealing at 773 K for 120 h; R_t is the average radius of Al₈CeCu₄ particles after annealing at a given temperature for a given time t ; K is a constant representing the ripening rate of the particles; D is the diffusion coefficient of the controlled element in the matrix; σ is the interfacial energy between the Al₈CeCu₄ phase and the matrix; R is universal gas constant

which is 8.314 J/K·mol; T is the absolute temperature of annealing; V_m and V_p are the mole volume of the matrix and Al_8CeCu_4 phase respectively, and C_m and C_p are the atomic concentration of the controlled element in the Al matrix and Al_8CeCu_4 phase respectively. The so-called controlled element indicates the one whose diffusion coefficient is the smallest and decides directly the rate of the ripening process.

The classical LSW equation is based on one hypothesis that the volume fraction of the second phase particles approaches to zero. However, the hypothesis hardly meets the industrial materials. Many researchers investigated the effect of the volume fraction of the second phase particles and drew a conclusion that the ripening rate of the second phase particles increased with the increase of its volume fraction^[15]. The influence of the second phase particles was quantitatively described by $K(\Phi)/K=A_1$, where $K(\Phi)$ represents the ripening rate of the particles for a given volume fraction Φ . Therefore, the Eq.(1) can be modified into the Eq.(2) for a given volume fraction of the particles:

$$R_t^3 - R_0^3 = Kt = A_1 D \sigma V_p^2 C_m / 9RTV_m C_p t \quad (2)$$

For Al-14Cu-7Ce alloy, the volume fraction of Al_8CeCu_4 particles is around 24%; therefore, A_1 is 3 according to the plot presented by the B-W relation^[15]. Consequently, Eq.(2) can be changed into Eq.(3):

$$R_t^3 - R_0^3 = Kt = 24D\sigma V_p^2 C_m / 9RTV_m C_p t \quad (3)$$

The mole volume V can be calculated by M/ρ , where, M and ρ is mole mass and volume density, respectively. For Al matrix, $M_{Al}= 27$ g/mol and $\rho_{Al}= 2.7$ g/cm³; for Al_8CeCu_4 , $M_{Al_8CeCu_4}= 610$ g/mol and $\rho_{Al_8CeCu_4}= 5.04$ g/cm³. Therefore, the mole volumes V_m and V_p for the matrix and Al_8CeCu_4 are 10 cm³/mol and 121 cm³/mol, respectively. Due to the little effect of temperature on the mole volume of the solid, V_m and V_p can be considered as a constant during kinetics calculation.

During annealing, the decrease of the hardness of Al-14Cu-7Ce alloy is closely relative to the growth of the average radius of Al_8CeCu_4 particles, which is controlled by the thermal activation process of atomic diffusion. Therefore, the change of the hardness can be described using the well-known general rate equation^[16], that is, the relation between the natural logarithm of the time, in which the initial hardness of the alloy decreases to the same level of the hardness, and the reciprocal of the annealing temperatures meets the linear relationship described as Eq.(4).

$$\ln t = A_2 + Q/RT \quad (4)$$

According to Eq.(4), the relationship between the natural logarithm of the annealing time and the reciprocal of the annealing temperature is shown in Fig.7. Here, the annealing time is adopted the value where the hardness $HV_{0.5}$ decreases from initial 835 MPa to 740 MPa (Fig.6), i.e. is 9, 19.9, 41.5 and 106.5 h. Using the linear fitting rule, the slope Q/R and the activation energy Q are determined to be 13.2 and 110.0 kJ/mol, respectively. The value of Q is smaller than the self-diffusion activation energy of Al ($Q_{Al}=142.3$ kJ/mol)^[17]

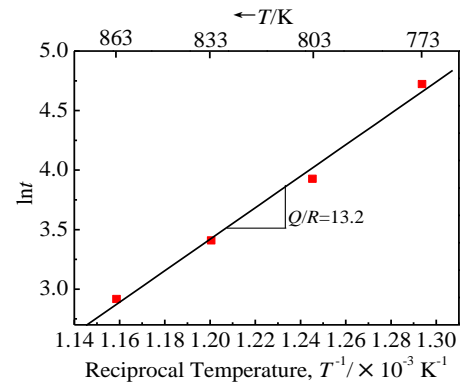


Fig.7 Plot of ln t vs 1/T

and the diffusion activation energy of Cu in the Al matrix ($Q_{Cu}=133.9$ kJ/mol)^[18], and close to the diffusion activation energy of Ce atom in the Al matrix ($Q_{Ce}=115.6$ kJ/mol)^[19].

According to the Arrhenius equation (5), the diffusion coefficient D of Ce atom in the Al matrix for different annealing temperatures can be calculated as shown in Table 1, where the diffusion constant D_0 is $6.683 \times 10^{-10} \text{ m}^2/\text{s}$ ^[20].

$$D = D_0 \exp(-Q/RT) \quad (5)$$

In order to determine the controlled element during the Ostwald ripening process of the Al_8CeCu_4 particles, we have calculated and compared the diffusion coefficient of Al, Cu and Ce atoms in the Al matrix at 863 K. The self-diffusion activation energy of Al $Q_{Al}=142.3$ kJ/mol and diffusion constant $D_{0Al}=1.7 \times 10^{-4} \text{ m}^2/\text{s}$; the diffusion activation energy of Cu atom in Al matrix $Q_{Cu}=133.9$ kJ/mol and diffusion constant $D_{0Cu}=4.4 \times 10^{-5} \text{ m}^2/\text{s}$. Therefore, the diffusion coefficient of Al and Cu atoms in the Al matrix at 863 K can be calculated, being $D_{Al}=4.14 \times 10^{-13} \text{ m}^2/\text{s}$ and $D_{Cu}=3.49 \times 10^{-13} \text{ m}^2/\text{s}$, respectively. These values are far larger than the diffusion coefficient of Ce atom in the Al matrix $D_{Ce}=1.475 \times 10^{-16} \text{ m}^2/\text{s}$. Therefore, Ce is considered as the controlled element during the Ostwald ripening process of the Al_8CeCu_4 particles in the Al-14Cu-7Ce alloy.

The atomic concentration of Ce, C_p , can easily be calculated to be 1/13 according to the molecular formula of Al_8CeCu_4 phase. According to the results given by Belov et al^[6], the solubility of Ce atom in the matrix, C_m , is about 0.01at% at 700 K. Generally, the solubility of one element tends to increase with the increase of temperature. Here, we suppose that the solubility of Ce atom in the Al matrix (C_m) increases linearly with the increase of annealing temperature and the calculated data C_m are shown in Table 1.

Table 1 Calculation results of parameters during Al_8CeCu_4 ripening process at different temperatures

T/K	$D/\text{m}^2 \text{ s}^{-1}$	C_m	$\sigma/\text{J m}^{-2}$
863	1.475E-16	0.0005	0.491
833	8.490E-17	0.0004	0.592
803	4.691E-17	0.0003	0.796
773	2.475E-17	0.0002	0.977

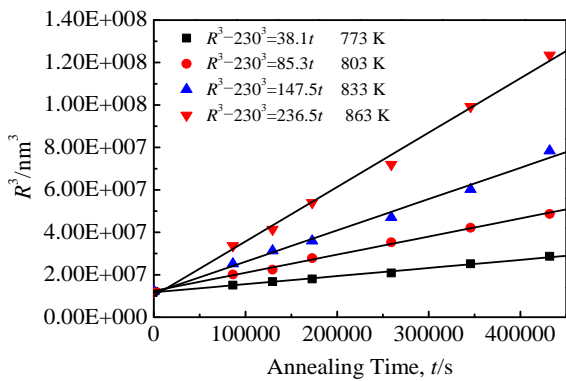


Fig.8 Curves of R^3-t of Al_8CeCu_4 particles annealed at different temperatures

Using the data of Fig.5, the values of the ripening rate $K(\Phi)$ can be calculated by linear fitting of the left side of Eq.(3), which are shown in Fig.8. According to the right side of Eq.(3), the values of the interfacial energy σ between the Al_8CeCu_4 particles and the matrix annealed at different temperatures have been calculated, which is also shown in Table 1.

3 Conclusions

1) The average radius of Al_8CeCu_4 particles in the Al-14Cu-7Ce alloy increases with the increase of annealing temperature and time, while the hardness of the alloy decreases with the increase of annealing temperature and time.

2) The Ostwald ripening process of Al_8CeCu_4 particles is controlled by the volume diffusion of Ce in the Al matrix.

3) Taking into account the effect of the volume fraction of Al_8CeCu_4 particles, the growth of the average radius of Al_8CeCu_4 particles satisfies the equation as following:

$$R_t^3 - R_0^3 = Kt = 24D\sigma V_p^2 C_m / 9RTV_m C_p t.$$

References

- 1 Park C H, Won J W, Park J W et al. *Metallurgical Materials Transaction A*[J], 2012, 43: 977
- 2 Poths R M, Wynne B P, Rainforth W M et al. *Metallurgical Materials Transaction A*[J], 2004, 35: 2993
- 3 Liu J T, Liu G Q, Hu B F et al. *Rare Metal Materials and Engineering*[J], 2006, 35(2): 418 (in Chinese)
- 4 Chen Y N, Wei J F, Zhao Y Q. *Rare Metal Materials and Engineering*[J], 2008, 37(4): 762 (in Chinese)
- 5 Cui B H, Guo J J, Su Y Q et al. *Acta Materllurgica Sinica*[J], 2007, 43(9): 907 (in Chinese)
- 6 Belov N A, Khvan A V. *Acta Materials*[J], 2007, 55: 5473
- 7 Bo H, Jin S, Zhang L G et al. *Journal of Alloys and Compounds* [J], 2009, 484: 286
- 8 Belov N A, Khvan A V, Alabin A N. *Materials Science Forum*[J], 2006, 519-521: 395
- 9 Huang L, Li H, Wang Z X et al. *Transaction of Materials and Heat Treatment*[J], 2012, 33: 60 (in Chinese)
- 10 Li W, Li H, Wang Z X et al. *Materials Science and Engineering A*[J], 2011, 528: 4098
- 11 Atasoy O E, Ozbilen S. *Journal of Materials and Science*[J], 1989, 24: 281
- 12 Polmear I J. *Materials Forum*[J], 2004, 28: 1
- 13 Lifshittz I M, Slyozov V V. *Journal of Physics and Chemistry of Solids*[J], 1961, 19: 35
- 14 Wagner C. *Zeitschrift für Elektrochemie*[J], 1961, 65: 581
- 15 Baldan A. *Journal of Materials and Science*[J], 2002, 37: 2171
- 16 Tian Y L, Kaft R W. *Metallurgical and Materials Transaction A*[J], 1987, 18: 1403
- 17 Lavernia E J, Ayers J D, Srivatsan T S. *International Materials Reviews*[J], 1992, 37: 1
- 18 Du Y, Chang Y A, Huang B et al. *Materials Science and Engineering A*[J], 2003, 363: 140
- 19 Cai W P. *Journal of Materials and Science Letters*[J], 1997, 16: 1824
- 20 Das S K, Davis L A. *Materials Science and Engineering A*[J], 1988, 98: 1

Al-14Cu-7Ce 合金中 Al_8CeCu_4 相的 Ostwald 熟化行为

李海^{1,2}, 许伟¹, 王芝秀^{1,2}, 方必军^{1,2}, 宋仁国^{1,2}, 郑子樵³

(1. 常州大学, 江苏 常州 213164)

(2. 江苏省材料表面科学与技术重点实验室, 江苏 常州 213164)

(3. 中南大学, 湖南 长沙 410083)

摘要: 采用硬度测试、扫描电镜、图像分析和物理建模, 研究了Al-14Cu-7Ce合金中 Al_8CeCu_4 相的Ostwald熟化行为。结果表明, Al_8CeCu_4 相的熟化过程受控于Ce元素在Al中的体扩散, 其动力学满足体积修正的Lifshits-Slyozov-Wagner理论; 基于通用速率公式, 计算了Ce元素在Al中的体扩散系数以及 Al_8CeCu_4 与Al基体的界面能。

关键词: Al-14Cu-7Ce; Al_8CeCu_4 ; Ostwald 熟化

作者简介: 李海, 男, 1972年生, 博士, 副教授, 常州大学材料科学与工程学院, 江苏 常州 213164, 电话: 0519-86330069,

E-mail: Lehigh_73@163.com